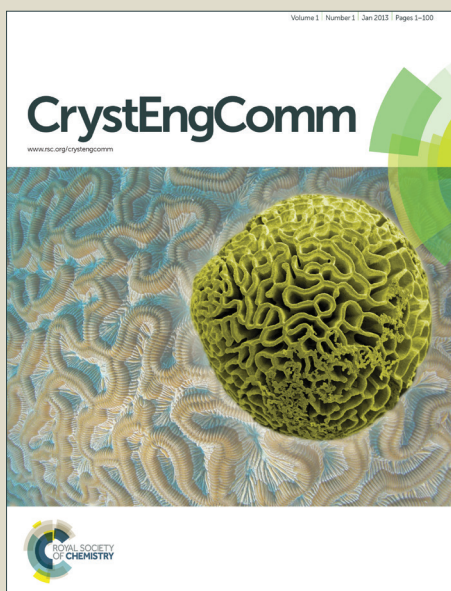


CrystEngComm

Accepted Manuscript



This is an *Accepted Manuscript*, which has been through the Royal Society of Chemistry peer review process and has been accepted for publication.

Accepted Manuscripts are published online shortly after acceptance, before technical editing, formatting and proof reading. Using this free service, authors can make their results available to the community, in citable form, before we publish the edited article. We will replace this *Accepted Manuscript* with the edited and formatted *Advance Article* as soon as it is available.

You can find more information about *Accepted Manuscripts* in the [Information for Authors](#).

Please note that technical editing may introduce minor changes to the text and/or graphics, which may alter content. The journal's standard [Terms & Conditions](#) and the [Ethical guidelines](#) still apply. In no event shall the Royal Society of Chemistry be held responsible for any errors or omissions in this *Accepted Manuscript* or any consequences arising from the use of any information it contains.

Solution-Mediated Phase Transformation of Uric Acid Dihydrate

Janeth B. Presores and Jennifer A. Swift*

Department of Chemistry, Georgetown University, 37th and O Sts., NW

Washington, DC 20057-1227

Abstract

Various crystalline phases of uric acid are frequently identified components of human kidney stones, including anhydrous uric acid (UA) and uric acid dihydrate (UAD). Herein we report a quantitative study of the solution-mediated phase transformation of metastable UAD to UA as a function of pH as well as in model urine solution. Using a combination of X-ray diffraction, thermal analysis, and optical microscopy techniques, the UAD to UA transformation was found to go to completion within 48 hours at 37° C in buffered solutions with pH between 4.0-6.5 with no evidence for intermediate crystalline phases. In solutions with pH > 6.8, UAD transformation to a different monosodium urate monohydrate phase becomes dominant. In artificial urine solution, the transformation occurs on a slightly faster timescale and results in smaller UA crystals. Seeding and saturation experiments indicate that the rate-limiting step in the overall transformation is the dissolution of UAD. The kinetics of these transformation processes suggest that interconversions between various solid state forms of uric acid are relevant under the physiologic conditions which lead to stone formation.

Introduction

Over 200 different crystalline materials have been identified in human kidney stones.^[1] The most abundant organic component is uric acid (Fig. 1), which is a product of protein metabolism. Uric acid exists in several different phases in physiologic deposits, including anhydrous (UA)^[2], monohydrate,^[3] and dihydrate (UAD)^[2] forms of uric acid, as well as sodium (MSU),^[4] calcium,^[5] potassium and ammonium^[6] salts of the ionized urate. Of these, UA is typically the most abundant phase, followed by the less stable UAD form. Interestingly, when UAD is present, it is almost always found in association with the anhydrous UA phase though not vice versa.^[2] Since UAD is metastable relative to UA,^[7] this observation raises the question of whether the UAD to UA transformation kinetics occur on a timescale relevant to kidney stone formation and if so, how various solution parameters affect the transformation process.

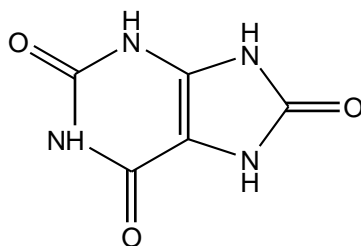


Fig. 1. Molecular structure of uric acid

Any phase transformation in solution is a complex process which must involve at least three key steps - dissolution of the metastable phase, and the nucleation and growth of the stable phase.^[8] A large number of phase transformation studies of other molecular crystal systems (polymorphic and hydrate/anhydrous systems) have been previously reported, which collectively indicate that any of these three steps can be rate-limiting.^[9] For example, the transformation kinetics of anhydrous carbamazepine to its more stable hydrate,^[10] was found to be dependent on the growth rate of the stable phase. In contrast, the dissolution rate of β -glycine is the rate-limiting step in its transformation to the more stable α form.^[9b] Collectively, these studies have also examined the influence of a variety of factors such as temperature, crystal size, solvent, agitation, lattice disorder, and the presence of seed crystals and/or additives on the transformation rates in a range of molecular crystal systems.

Solution-mediated phase transformation processes may also operate under physiologic conditions leading to kidney stone formation. Calcium oxalate forms three hydrates - a thermodynamically stable monohydrate, and a metastable dihydrate and trihydrate. Batch precipitation experiments^[11] suggest the dihydrate to monohydrate transformation is a solution-mediated process. Qualitative observations of UAD transformation to UA in aqueous and artificial urine solutions have also been previously reported.^[12] Boistelle *et al.*^[12a] observed that aqueous suspensions of UAD crystals turn opaque and UA crystals are observed to grow epitaxially on UAD crystal surfaces. *In vitro* studies by Grases *et al.*^[12b] showed that UAD precipitated from artificial urine transformed to UA in two days. However, more quantitative analyses of the phase composition of the crystalline suspensions with respect to time and the effects of key solution parameters such as pH have not been reported.

We previously reported^[7] a quantitative mechanistic and kinetic study of the UAD to UA phase transformation in air as a function of particle size and relative humidity. However, phase transformations in solution and air are mechanistically quite different. The current study is a quantitative investigation of the UAD to UA transformation kinetics under aqueous conditions controlling for pH and ionic strength, as well as in artificial urine solution. All phase transformation studies were carried out at 37° C and monitored with a combination of optical microscopy, powder X-ray diffraction (PXRD), and thermogravimetric analysis (TGA) techniques. The timescale of the process suggests that metastable UAD precipitated under physiologic conditions is an important intermediate in the pathology of uric acid stones, regardless of whether the UAD phase is present in the final renal deposit.

Experimental Section

Materials. All chemical reagents were used as received without further purification. Water was purified by passage through two Barnstead deionizing cartridges followed by distillation. Uric acid solutions of pH 4 were prepared from uric acid (>99%, Sigma), sodium acetate (99% EMD), and acetic acid (99.7%, EMD). McIlvaine buffers^[13] with controlled pH and ionic strength were prepared from C₆H₈O₇·H₂O (99.0%, EMD), Na₂HPO₄ (99.5%, Fisher), and KCl (99.0%, Sigma). Artificial urine solution was prepared from an established recipe^[14]

based on mixtures of Na₂SO₄ (99.9%, Sigma), KCl (99.0%, Sigma), NH₄Cl (99.8%, EM Science), MgSO₄·7H₂O (98-102%, EM Science), Na₂HPO₄ (99.5%, Fisher), NaH₂PO₄·H₂O (99.1%, Fisher), NaCl (99%, EM Science), Na₃C₆H₅O₇·2H₂O (Certified, Fisher), and urea (Certified ACS, Fisher).

UAD Crystal Growth. Pure crystals of UAD were grown by dissolving 180-200 mg of uric acid in 1 L boiling distilled water. The pH of the solution was buffered to 4.0 with sodium acetate and acetic acid and maintained at 25° C for 48 hours. UAD crystals were vacuum-filtered and briefly air-dried. Most crystals were ~100 μm rectangular plates with large (001) faces and smaller (102) and (011) side faces. Freshly grown unground UAD samples were used immediately in phase transformation studies, since grinding and/or prolonged exposure to air can lead to premature ~1% water loss.

UAD to UA Transformation. Approximately 20 mg of unground UAD was added to 24 glass bottles each containing 50 mL of pH 4 McIlvaine buffer solutions (Ionic Strength, IS = 0.5 M). The suspensions were placed in a 37° C water bath. Three bottles were removed from the bath in regular 6 h time intervals for a period of 48 h, and the solid phase was vacuum-filtered, washed with distilled water, air-dried and immediately subjected to microscopy, TGA and PXRD analysis. The transformation of UAD was similarly performed in pH 5, 6, 6.8, and 7 McIlvaine buffer solutions (IS = 0.5 M) as well as artificial urine solution. The effect of seeding on the transformation of UAD to UA in artificial urine solution was evaluated by adding 10% (w/w) anhydrous uric acid powder to the starting solution. In a different experiment, 20 mg UAD crystals were added to 50 mL artificial urine solution saturated with uric acid and the UAD transformation was monitored for 48 hours.

Optical Microscopy. The morphology and size of the crystals were examined with an Olympus BX-50 polarized optical microscope fitted with a Nikon COOLPIX995 digital camera operated with krinnicam_v1-03 software (Nikon Corp.).

Thermal Analysis. Thermogravimetric analyses (TGA) were performed on a SDT Q600 TA instrument (New Castle, DE). All experiments were conducted in at least triplicate using

open 90 μL alumina pans (TA instruments) and heated from room temperature to 150° C at 10° C/min under a nitrogen stream with a flow rate of 50 mL/min. All experimental curves were analyzed with TA's Universal Analysis Software. The calculated weight loss of pure UAD dehydration is 17.65%. The % UAD to UA conversion was determined by the difference method.

Powder X-ray Diffraction. Powder X-ray diffraction was performed using a Rigaku R-AXIS RAPID-S X-ray diffractometer under the following conditions: tube voltage of 40kV, tube current of 30 mA, and Cu $K\alpha$ radiation. The samples were scanned in steps of 0.01° over a 2θ range of 4° to 50° at a speed of 0.1°/sec with a total scan time of 60 min. Data analysis was performed using Jade v5.035 software (Material Data Inc.). Since sample grinding may contribute to the premature dehydration of UAD, PXRD analyses were performed on unground samples. The transformation of UAD to UA was tracked by the appearance and disappearance of several characteristic diffraction lines in specific 2θ regions where there is little or no overlap between UAD and UA reflections. Intense diffraction lines for UAD are (002), (011), (102), (004), (112), (210), and (21-1) while that for UA are (200), (001), (210), (11-1), (121), and (021).

Results and Discussion

The mechanism for the transformation from a metastable to a stable form in solution involves the dissolution of the metastable form, the nucleation of the stable form, and growth of the stable form. Solubility differences typically serve as the driving force for such transformations. The solubility of uric acid has been the subject of previous studies^[15] in order to elucidate the process of uric acid stone formation as well as to understand oral dissolution therapies. Uric acid exhibits poor solubility in most aqueous solutions, though the metastable UAD is more soluble than UA. At 37° C, UAD has an aqueous solubility (0.63 mM) about twice that of UA (0.31 mM).^[15a]

The solubilities of UAD and UA are independent of pH when $\text{pH} \leq 3$, but at higher solution pH, uric acid dissociates to form urate ($\text{pK}_a = 5.5$ ^[16]). At higher pH values, the total concentration is the sum of the uric acid and urate concentrations in solution. Urate can also

deprotonate to diurate at higher pH ($\text{pK}_{\text{a}2} = 10.3$), but under physiologically relevant conditions the contribution of diurate is negligible. The solubility of uric acid in standard reference artificial urine is the same as that in aqueous solutions with ionic strengths ranging from 0.15 - 0.30 M.^[15b] This holds true regardless of the nature and concentration of the inorganic urine components and/or the presence of organic substances like urea and creatine.^[15b]

The crystal structures of both UA^[17] and UAD^[18] are also both known. In the UA structure ($P2_1/a$: $a = 14.464(3)$, $b = 7.403(2)$, $c = 6.208(1)$ Å, and $\beta = 65.10(5)^\circ$), uric acid molecules hydrogen bond head-to-head and tail-to-tail into 1D ribbons which align parallel to one another in the bc plane. Molecules in adjacent bc layers also hydrogen bond to one another. In the UAD structure ($P2_1/c$: $a = 7.237(3)$ Å, $b = 6.363(4)$ Å, $c = 17.449(11)$ Å, and $\beta = 90.51(1)^\circ$), nearly identical layers of parallel ribbons form in the ab plane, although these layers are hydrogen bonded to and separated by water molecules. The similarity in the two structures is clear when comparing the lattice dimensions of the UA (100) (7.4×6.2 Å, 90°) and UAD (001) (7.2×6.3 Å, 90°) planes. Crystal packing diagrams of both UAD and UA viewed along 2 crystallographic axes each, are found in the Supplementary Info (Fig. S1 and S2).

Transformation in buffered solutions at 37° C. UAD crystals grown from pH = 4 solution at room temperature were harvested from solution and immediately added to 37° C McIlvaine buffer solution (IS = 0.5M). The transformation was then monitored in 6 h intervals over a period of 48 h. The photomicrographs in Fig. 2 are representative of the typical transformation from UAD to UA at pH 4. Initially the solution consists of clear colorless UAD plates, but within even the first few hours, as these plates begin to dissolve, the surfaces roughen and the crystals begin to lose their transparency. Often crystals of the UA phase are found growing on the surfaces of these dissolving UAD crystals. The micrographs taken at 12-24 hours showed a mixture of clear and opaque UAD crystals as well as the newly formed small UA. Close examination of the micrograph at 18 hours reveals epitaxial nucleation of UA on the surface of roughened UAD. This heterogeneous nucleation is in accordance with previous reports of epitaxial matches between (001) UAD and (100)

UA.^[12a, 19] As the growth of the anhydrous phase continued, UAD was consumed as shown by the smooth UA crystals observed at 42 to 48 hours. Individual UA and UAD crystals can be distinguished by light interference microscopy as described elsewhere.^[20] Sequential images of the transformation in buffered solutions with pH = 5, 6 and 6.5 look qualitatively similar.

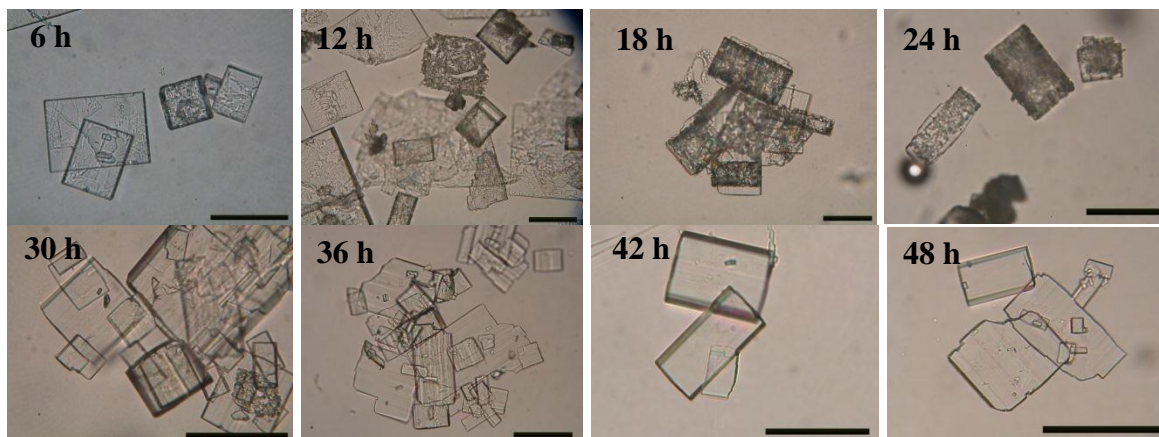


Fig. 2. Representative photomicrographs of samples harvested from solution at different times during the phase transformation of UAD to UA in pH 4 McIlvaine buffer at 37° C. Individual crystals can be identified as UAD or UA using light interference microscopy. Scale bar = 100 μm .

The phase composition of the samples was examined by PXRD. Since grinding UAD samples can contribute to their premature dehydration,^[7] all PXRD analyses were performed on unground samples. This results in some preferred orientations, but still allows for clear identification of UAD and UA phases. PXRD patterns collected on crystals suspended in pH 4 are found in Fig 3. The transformation of UAD was marked by the appearance and disappearance of several characteristic diffraction lines. The diffraction pattern at 6 h showed reflections corresponding mostly to UAD, including characteristic ones at (002), (004) and (112). Starting at 12 h, distinct (200), (210), (11-1) UA reflections appear. Both UAD and UA are clearly present in the mixture between 12-36 h. The decreasing intensity and subsequent disappearance of these UAD diffraction lines coincided with the appearance of strong UA (200), (210), and (11-1) reflections. By 42-48 h, the only visible diffraction lines corresponded to UA, indicating that the transformation was complete.

PXRD taken at 6 h intervals during the transformation in pH = 5 and 6 McIlvaine buffer were qualitatively identical. In general, diffraction lines for UAD took just slightly longer to disappear in samples harvested from pH 6 solutions. No intense peaks other than those ascribable to UA or UAD phases were ever observed, which suggests that the UAD to UA transformation likely involves no intermediate crystalline phases. These results were consistent with previous work by Ringertz,^[21] who asserted that UAD dehydration leads directly to polycrystalline UA.

Quantifying the extent of UAD transformation was more readily and accurately accomplished with thermogravimetric analysis (TGA) of the solid phase removed from solution at the same regular time intervals. UAD is 17.64% water by weight. With only dihydrate and anhydrous phases present in partially transformed samples, the difference method could be used to calculate the % UA at any given time. The % conversion to UA in pH = 4, 5 and 6 McIlvaine solutions is summarized in Fig. 4. All measurements were done in at least triplicate, and the standard deviations at each time point are indicated. Although the transformation times are slightly different, the shapes of the transformation profiles at the three pH investigated are quite similar. All seem to show an induction time is required, presumably to initially saturate the buffer solution with uric acid. Optical micrographs over the same time period also show characteristic roughening of the UAD surfaces as the crystals initially dissolve. Similar transformation rates are observed up to 24 hours at pH 4, 5, and 6. At pH 4 and 5, a fast acceleration and leveling off are observed showing a ~97% conversion of UAD to UA at 36 hours. At pH 6, the transformation rate is more continuous and only 75% conversion at 36 hours. The decreased rate at higher pH was initially counterintuitive because UAD solubility increases with pH. However, at pH = 6, a majority of uric acid molecules in solution are deprotonated though there was no evidence for urate phases in the PXRD at pH 6.



Fig. 3. PXRD patterns of the transformation of UAD to UA in pH 4 McIlvaine buffer at 37° C. The diffraction pattern at 6 h showed reflections corresponding mostly to UAD. At 12-36 h, both UAD and UA were present. By 42-48 h, diffraction lines corresponded exclusively to UA, indicating that the transformation was complete.

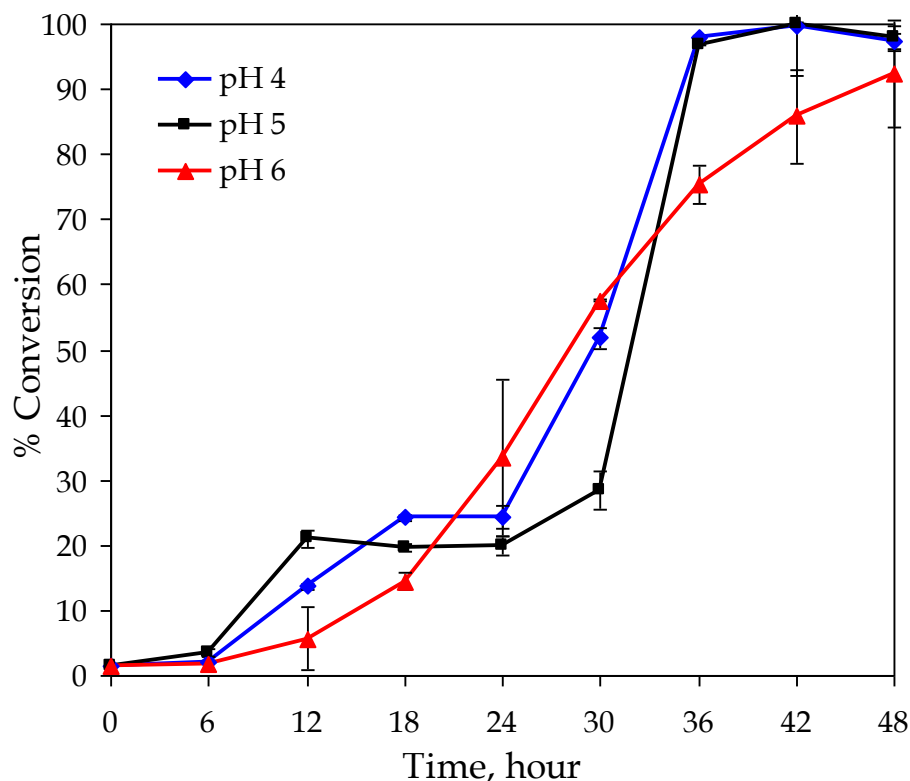


Fig. 4. Summary of the % conversion of UAD to UA as a function of time in McIlvaine buffer solutions. All experiments were performed in triplicate and error bars of the standard deviation are shown. Blue curve = pH 4, Black curve = pH 5, Red curve = pH 6.

As the solution pH was increased to 6.8, the transformation rate slows further; only ~20-25% of the initial UAD has undergone conversion to UA between 18 and 36 h. Micrographs of the sample taken after 42 h show a mixture of plate-like and needle-like crystals (Fig. 5). The TGA for this mixture shows two distinct weight loss steps. The first weight loss at $<100^{\circ}\text{C}$ is consistent with water loss from UAD, and the second weight loss was observed from 150°C to 250°C . This second weight loss corresponds to water loss from monosodium urate monohydrate (MSU), a stable hydrate at RT. The fine needle morphology and PXRD were also consistent with MSU formation.

Just a slight increase in the solution pH to 7 significantly accelerated the transformation to MSU (Fig. 6, and Supplementary Info S3). The dark and rough appearance of some of the plates at 12 h suggested that some dehydration to UA and/or dissolution

occurred (TGA showed ~19% less water loss from the sample relative to what is expected for pure UAD), however, PXRD showed UAD exclusively. No diffraction lines corresponding to UA or MSU could be distinguished from the baseline PXRD at that time. We can not unambiguously rule out the possibility that a 3-step transformation from UAD to UA to MSU occurs, but it seems more likely that UAD dissolution is followed by the direct precipitation of MSU. The composition was quite different by 18 h, with both optical microscopy and PXRD showing exclusively MSU. The needle-like crystals produced in the transformation process were identical to MSU crystals grown in uric acid solutions with $\text{pH} > 7$.^[22] No additional phase changes were observed up to 48 h later.



Fig. 5. Photomicrograph of the transformation of UAD in pH 6.8 McIlvaine buffer at 37° C, taken after 42 hours. Scale bar = 100 μm .

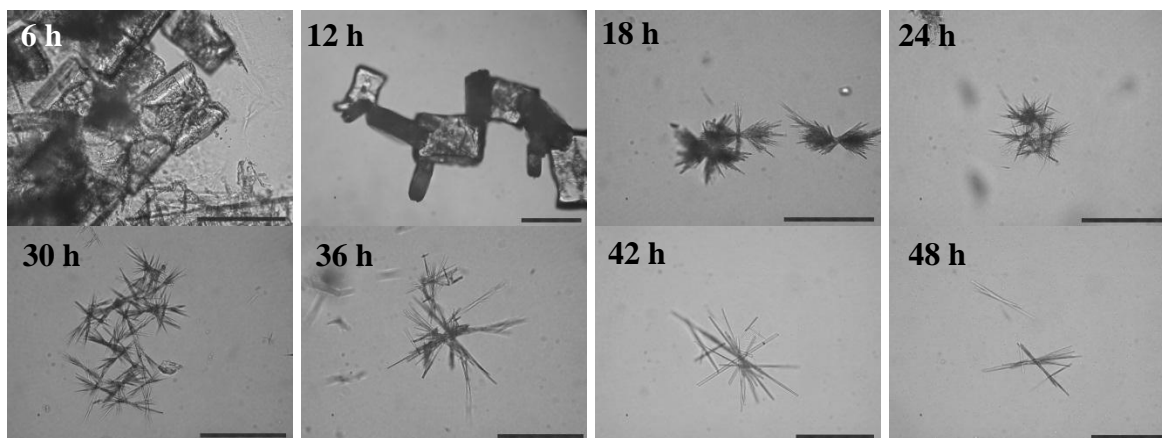


Fig. 6. Representative photomicrographs of samples harvested from solution at different times during the phase transformation of UAD in pH 7 McIlvaine buffer at 37° C. By 18 h, only needles of MSU are apparent. Scale bar = 100 μm .

Transformation in artificial urine solution. To more closely mimic UAD transformation under physiological conditions, similar experiments were performed in artificial urine. Model urine solution was prepared according to established recipe by dissolving various salts in an aqueous solution.^[14] The urine solution contains no other molecular or macromolecular or components, but has a pH ~5 and an ionic strength similar to the buffer solution. Grases *et al.*^[12b] previously reported that UAD converts to UA in urine, however, in the present study we build on this observation by examining the solid state composition at select time intervals, and also investigate the effect of seeding on the transformation rate.

The optical micrographs in Fig. 7 follow the transformation of UAD in artificial urine over 48 h. Qualitatively the transformation in urine looks similar to that in buffer, except that both UAD and UA crystals have more rounded edges and the product UA crystals tend to be smaller in size in artificial urine. PXRD data collected every 6 h throughout the transformation are shown in Fig 8. All diffraction patterns collected between 6-24 h show the presence of both UAD and UA, but only UA from 30 h on. There were no unassignable reflections that would indicate the presence of any other intermediate or stable crystalline phases. The transformation rates in buffer and urine can be directly compared by examining the black lines in Fig. 4 (pH 5 buffer) and Fig 9 (urine). Not only does the conversion to UA in urine clearly occur faster (transformation is complete in 30 h vs 42 h in buffer), but it proceeds at a more constant rate throughout and does not exhibit any appreciable induction time. This is perhaps not surprising given the comparatively higher solubility of uric acid in urine relative to water.

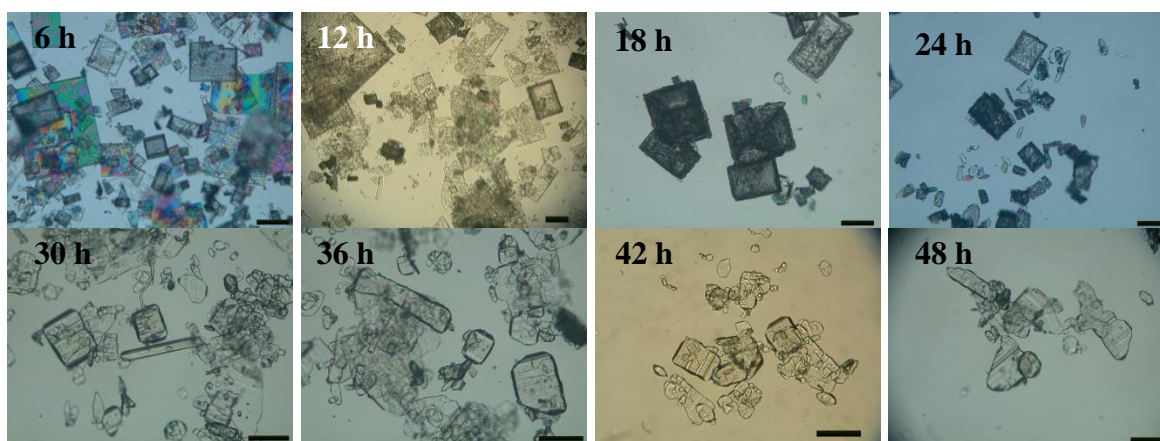


Fig. 7. Representative photomicrographs of samples harvested from solution at different times during the phase transformation of UAD to UA in artificial urine at 37° C. Scale bar = 100 μm .

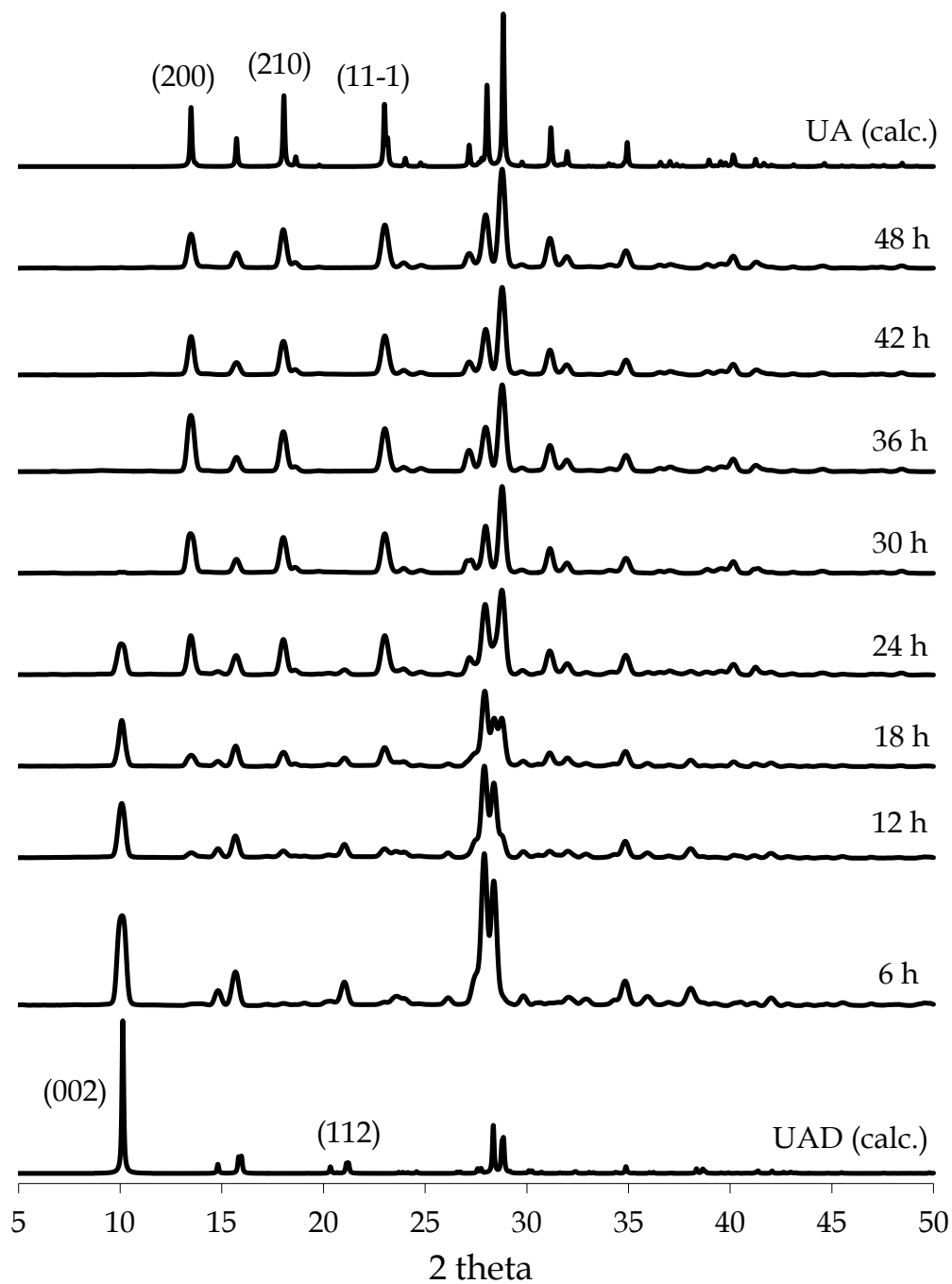


Fig. 8. PXRD patterns of the transformation of UAD to UA in artificial urine solution at 37° C, pH ~5. The diffraction patterns at 6-24 h showed reflections corresponding to both UAD and UA. Starting at 36 h, diffraction lines corresponded to UA indicating that the transformation was complete.

This raised question as to whether the rate limiting step in the transformation was determined by the dissolution of the initial UAD phase, or the nucleation and/or growth of the product UA phase. We sought to elucidate this through two key experiments. In the first, 10 % (w/w) of anhydrous uric acid powder was added to the initial solution. Transformation in the seeded solutions (blue curve, Fig. 9) showed a two-fold increase in the transformation at 6 h, though the time to effect complete transformation remained the same as in the absence of seeds. This effectively ruled out UA nucleation as the rate limiting step. Next, the transformation was examined in urine that was pre-saturated with dissolved uric acid. Since the solution is already saturated with uric acid, UAD does not dissolve as readily compared to other experiments. The UAD conversion occurred more slowly in this pre-saturated solution, requiring a full 48 h to completely transform to UA (red line, Fig. 9). This result confirmed that the initial dissolution of UAD must be the rate limiting step in the overall transformation.

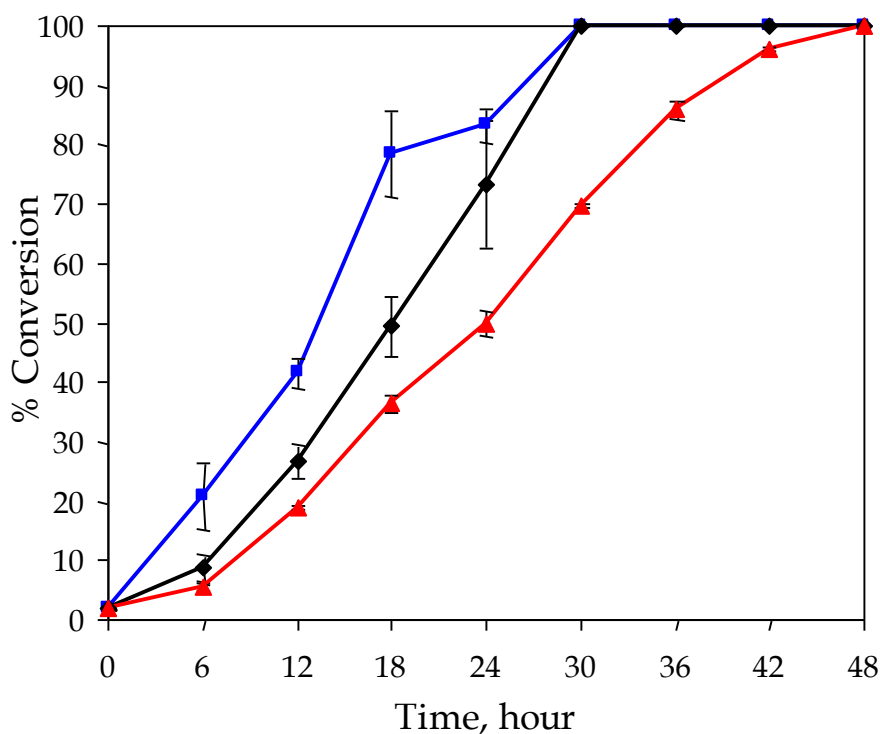


Fig. 9. Transformation of UAD in artificial urine solution at 37° C. All experiments were performed in triplicate and error bars of the standard deviation are shown. (Blue) UAD seeded with 10% (w/w) UA in artificial urine solution; (Black) UAD in artificial urine solution; (Red) UAD in artificial urine solution saturated with uric acid.

Conclusion

The conversion of UAD to UA occurs via a dissolution and recrystallization, and was monitored in real time using a combination of optical microscopy, powder X-ray diffraction and thermogravimetric analysis. In 37° C McIlvaine buffer over a pH range of 4-6.5, the UAD to UA transformation occurred via a dissolution and recrystallization mechanisms with no indication of other metastable intermediates. The transformation rates at pH 4 and 5 were nearly identical, and are characterized by a slow induction time followed by a rapid rate increase until the process reaches completion at ~42 h. In stark contrast, UAD in buffer with higher pH (6.8 – 7) transforms to the stable MSU salt either directly or via a UA intermediate.

The UAD to UA transformation at 37° C in model urine revealed a similar dissolution and recrystallization mechanism by optical microscopy, although the final UA crystals were typically smaller and had less well defined faces compared to those recrystallized in buffer. Although the buffer and urine have equivalent pH and ionic strengths, transformation in urine occurred at a faster and more consistent rate, reaching completion in 30h. Seeding and saturation experiments indicated that the rate limiting step in the transformation process is the dissolution of the starting UAD phase. Notably, the solution-mediated transformation of UAD to UA is several orders of magnitude faster than the corresponding dehydration reaction in air.^[7] The timescale of the dissolution-recrystallization process under model physiologic conditions provides a viable explanation for why UAD is rarely found in the

physiologic deposits in the absence of UA.^[1a] With the phase-transformation kinetics in model solutions now established, future studies can more specifically seek to address how individual molecular and macromolecular urinary components and/or designer additives alter the growth of UAD as well as its transformation to the more stable UA phase.

Acknowledgments

We gratefully acknowledge financial support provided by the National Science Foundation (CHE-0809684, DMR-1306247).

References

- [1] a) L. Herring, *Journal of Urology* **1962**, *88*, 545-562; b) D. Bazin, M. Daudon, C. Combes and C. Rey, *Chemical Reviews* **2012**, 5092-5120.
- [2] K. Lonsdale and P. Mason, *Science* **1966**, *152*, 1511-1512.
- [3] G. Schubert, G. Reck, H. Jancke, W. Kraus and C. Patzelt, *Urological Research* **2005**, *33*, 231-238.
- [4] N. S. Mandel and G. S. Mandel, *J. Am. Chem. Soc.* **1976**, *98*, 2319-2323.
- [5] J. B. Presores, K. E. Cromer, C. Capacci-Daniel and J. A. Swift, *Crystal Growth & Design* **2013**, *13*, 5162-5164.
- [6] V. B. Pichette, A.; Cardinal, J.; Houde, M.; Nolin, L.; Boucher, A.; Ouimet, D., *J. Kidney Diseases* **1997**, *30*, 237-242.
- [7] A. Z. Zellelow, K.-H. Kim, R. E. Sours and J. A. Swift, *Cryst. Growth Des.* **2010**, *10*, 418-425.
- [8] a) P. T. Cardew and R. J. Davey, *Proc. R. Soc. Lond. A* **1985**, *398*, 415-428; b) R. J. Davey and P. T. Cardew, *J. Cryst. Growth* **1986**, *79*, 648-653.
- [9] a) D. Murphy, F. Rodríguez-Cintrón, B. Langevin, R. C. Kelly and N. Rodríguez-Hornedo, *International Journal of Pharmaceutics* **2002**, *246*, 121-134; b) E. S. Ferrari, R. J. Davey, W. I. Cross, A. L. Gillon and C. S. Towler, *Crystal Growth & Design* **2003**, *3*, 53-60; c) S. Dharmayat, R. B. Hammond, X. Lai, C. Ma, E. Purba, K. J. Roberts, Z.-P. Chen, E. Martin, J. Morris and R. Bytheway, *Crystal Growth & Design* **2008**, *8*, 2205-2216; d) T. N. P. Nguyen and K.-J. Kim, *AIChE J.* **2011**, *1*, 1-10; e) T. Mukuta, A. Y. Lee, T. Kawakami and A. S. Myerson, *Crystal Growth & Design* **2005**, *5*, 1429-1436; f) N. Rodríguez-Hornedo, D. Lechuga-Ballesteros and H.-J. Wu, *Int. J. Pharm* **1992**, *85*, 149-162; g) T. Ono, J. H. ter Horst and P. J. Jansens, *Crystal Growth & Design* **2004**, *4*, 465-469; h) R. C. Kelly and N. Rodríguez-Hornedo, *Org. Process Res. Dev.* **2009**, *13*, 1291-1300; i) H. Wikström, J.

- Rantanen, A. D. Gift and L. S. Taylor, *Crystal Growth & Design* **2008**, *8*, 2684-2693; j) J. Schöll, D. Bonalumi, L. Vicum, M. Mazzotti and M. Müller, *Crystal Growth & Design* **2006**, *6*, 881-891; k) R. Mohan, K.-K. Koo, C. Strege and A. S. Myerson, *Ind. Eng. Chem. Res.* **2001**, *40*, 6111-6117; l) R. I. Petrova, A. Peresypkin, C. J. Mortko, A. E. McKeown, J. Lee and J. M. Williams, *Journal of Pharmaceutical Sciences* **2009**, *98*, 4111-4118.
- [10] H. Qu, M. Louhi-Kultanen, J. Rantanen and J. Kallas, *Crystal Growth & Design* **2006**, *6*, 2053-2060.
- [11] L. Brečević, D. Škrtić and J. Garside, *Journal of Crystal Growth* **1986**, *74*, 399-408.
- [12] a) R. Boistelle and C. Rinaudo, *J. Cryst. Growth* **1981**, *53*, 1-9; b) F. Grases, A. I. Villacampa, A. Costa-Bauzá and O. Söhnel, *Clin. Chim. Acta* **2000**, *302*, 89-104.
- [13] D. D. Perrin and B. Dempsey, *Buffers for pH and Metal Ion Control*, John Wiley & Sons, New York, **1974**, p.153.
- [14] L. C. Isaacson, *Invest. Urol.* **1969**, *6*, 356-363.
- [15] a) E. Königsberger and L.-C. Königsberger, *Pure Appl. Chem.* **2001**, *73*, 785-797; b) E. Königsberger and Z. Wang, *Monatsh. Chem.* **1999**, *130*, 1067-1073.
- [16] R. C. Smith, J. Z. Gore, M. McKee and H. Hargis, *Microchemical Journal* **1988**, *38*, 118-124.
- [17] H. Ringertz, *Acta. Cryst.* **1966**, *20*, 397-403.
- [18] S. Parkin and H. Hope, *Acta. Cryst.* **1998**, *B54*, 339-344.
- [19] R. E. Sours and J. A. Swift, *ACA Trans.* **2004**, *39*, 83-89.
- [20] R. E. Sours, D. A. Fink and J. A. Swift, *J. Am. Chem. Soc.* **2002**, *124*, 8630-8636.
- [21] H. Ringertz, *Acta. Cryst.* **1965**, *19*, 286-287.
- [22] C. M. Perrin, M. A. Dobish, E. Van Keuren and J. A. Swift, *CrystEngComm* **2011**, *13*, 1111-1117.